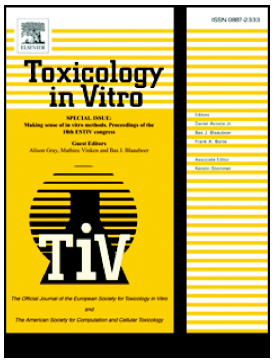

Evaluation of toxicity of heated tobacco products aerosol and cigarette smoke to BEAS-2B cells based on 3D biomimetic chip model

Hongjuan Wang, Fengjun Lu, Yushan Tian, Sen Zhang, Shulei Han, Yaning Fu, Jun Li, Pengxia Feng, Zhihao Shi, Huan Chen, Hongwei Hou

PII: S0887-2333(23)00157-1

DOI: https://doi.org/10.1016/j.tiv.2023.105708

Reference: TIV 105708

To appear in: *Toxicology in Vitro*

Received date: 23 May 2023

Revised date: 28 August 2023

Accepted date: 3 October 2023

Please cite this article as: H. Wang, F. Lu, Y. Tian, et al., Evaluation of toxicity of heated tobacco products aerosol and cigarette smoke to BEAS-2B cells based on 3D biomimetic chip model, *Toxicology in Vitro* (2023), https://doi.org/10.1016/j.tiv.2023.105708

Evaluation of Toxicity of Heated Tobacco Products Aerosol and Cigarette Smoke to BEAS-2B cells Based on 3D Biomimetic Chip Model

Hongjuan Wang[a,b,c,d,1], Fengjun Lu[a,b,1], Yushan Tian[a,b,c,d], Sen Zhang[e], Shulei Han[a,b,c,d], Yaning Fu[a,b,c,d], Jun Li[a,b,c,d], Pengxia Feng[a,b], Zhihao Shi[a,b], Huan Chen[a,b,c,d], Hongwei Hou[a,b,c,d]

[a]China National Tobacco Quality Supervision &Test Center, Zhengzhou, China

[b]Key Laboratory of Tobacco Biological Effects, Zhengzhou, China

[c]Beijing Institute of Life Science and Technology, Beijing, China

[d]Key Labortory of Tobacco Biological Effects and Biosynthesis, Beijing, China

[e]Shaanxi Key Laboratory of Degradable Biomedical Materials, School of Chemical Engineering, Northwest University, Xi'an 710069, China

* Corresponding authors:

Dr Huan Chen, E-mail: hunny_ch@163.com

Dr Hongwei Hou, E-mail: qsfctc@163.com

Tel./Fax: +86-0371-67672261

Postal address: No.6, Cuizhu Street, Gaoxin District, Zhengzhou, 450001, P.R. China.

E-mail: Hongjuan Wang (redbri2013@163.com), Fengjun Lu (18749677132@163.com), Yushan Tian (yushantian@126.com), Sen Zhang (zhsn@nwu.edu.cn), Shulei Han (hsl1983@163.com), Yaning Fu (fynmail@126.com), Jun Li (lijun@tbescience.com), Pengxia Feng(787797309@qq.com), Zhihao Shi (490976733@qq.com), Huan Chen (hunny_ch@163.com), Hongwei Hou (qsfctc@163.com)

ABSTRACT

It is still a controversial topic about evaluating whether heated tobacco products

(HTP) really reduce harm, which involves the choice of an experimental model. Here, a three-dimensional (3D) biomimetic chip model was used to evaluate the toxicity of aerosols came from HTP and smoke produced by cigarettes (Cig). Based on cell-related experiments, we found that the toxicity of Cig smoke extract diluted four times was also much higher than that of undiluted HTP, showing higher oxidative stress response and cause mitochondrial dysfunction. Meanwhile, both tobacco products all affect the tricarboxylic acid cycle (TCA), which is manifested by a significant decrease in the mRNA expression of TCA key rate-limiting enzymes. Summarily, 3D Biomimetic chip technology can be used as an ideal model to evaluate HTP. It can provide important data for tobacco risk assessment when 3D chip model was used. Our experimental results showed that HTP may be less harmful than tobacco cigarettes, but it does show significant cytotoxicity with the increase of dose. Therefore, the potential clinical effects of HTP on targeted organs such as lung should be further studied.

Key words: Chip Model; Cigarette smoke; Heated Tobacco Products; Inflammation; Mitochondrion; Tricarboxylic Acid Cycle

Introduction

Toxicological assessment is mostly carried out through animal experiments, and the data generated can be used as a reliable basis for its potential risk assessment. However, many studies have confirmed that although animal models provide complex physiological structures and controllable experimental environments that very alike human cells and organ systems, animal experiments have limited the prediction of the toxicity of compounds in humans due to the huge differences between species (Doke and Dhawale, 2015; Robinson et al., 2019; Wallace Hayes et al., 2020). Furthermore, the emphasis on animal ethics (3Rs principle of animal experimentation) in the field of scientific research has also made the use of animal models more cautious, so in vitro alternative models have attracted more and more attention.

Traditional monolayer cell culture systems can't fully reflect the physiological environment of real tissues, which even changed tissue-specific structures, mechanical/biochemical signals and intercellular communication (Oh et al., 2022; Yamada and Cukierman, 2007). The three-dimensional cell culture developed on the basis of two-dimensional (2D) cell culture solves the above problems well. The "organ chip (chip model)" is a microfluidic cell culture device fabricated by microchip manufacturing method. By reconstructing the human multi-cell structure, tissue-tissue interface, physical and chemical microenvironment and blood perfusion on the chip (Nahak et al., 2022; Ramadan and Gijs, 2015; Shuler, 2017), organ chips can produce levels of tissue and organ function that cannot be achieved by traditional 2D or 3D culture systems (Cukierman et al., 2001; Mazzoleni et al., 2009).

There have been many experiments based on chip models for toxicity evaluation, among which tobacco safety accounts for a large part. It is well known that more than 4000 compounds are produced in cigarette smoke (Berkowitz et al., 2018; Fricker et al., 2018; Kennedy-Feitosa et al., 2019), and different compounds have different effects on different types of tissue cells. Hou et al. constructed a lung-on-a-chip model

based on lung epithelial cells and vascular endothelial cells and evaluated the potential hazards of cigarette (Cig) smoke exposure (Hou et al., 2020). The results showed that the level of inflammatory factor TNF-α/IL-6 increased. Carnevali et al. evaluated the toxicity of cigarette smoke extract (CSE) based on a human lung fibroblast cell line (HFL-1) chip and found that CSE dose-dependently induced apoptosis and oxidative stress (Carnevali et al., 2003). Marinucci et al exposed human gingival fibroblasts (BSCL138) and human oral keratinocytes (PSC-200-014) to CSE, e-CSE, and HTP aerosol extract to explore the different biological effects (Marinucci et al., 2022). The experimental results showed that undiluted tobacco smoke extract significantly inhibited cell viability and cell migration, caused cell morphological changes and induced cell death. No change or damage was observed after e-CSE extract treatment. HTP extracts induced cell proliferation, manifested as increased cell viability, cell migration and cycle analysis changes. Hoshino et al exposed A549 cells to CSE and found that 5 % concentration could induce apoptosis and necrosis (Hoshino et al., 2001). In vitro experiments (chip model) have confirmed that CSE can increase the expression and secretion of IL-8 in human bronchial epithelial cells, both primary and tumor-derived NCI-H292 cell lines (Mio et al., 1997; Richter et al., 2002). Similar results were found in electronic toxicology evaluation based on chip technology. Studies have shown that e-cigarette extract (eCVE) leads to decreased lactate dehydrogenase activity (Cervellati et al., 2014), increased MMP-9 and IL-8 release (Higham et al., 2016). The toxicological evaluation of traditional cigarettes and E-cigarettes has confirmed the unique advantages of organ chips. However, we still have not found the research progress of using the above technology to evaluate heated tobacco products (HTP). Although some scientific studies have shown that HTP significantly reduce the content of harmful components in smoke, there is still a lack of sufficient evidence to show that HTP do real risk reduction (Başaran et al., 2019; McKelvey et al., 2018a; McKelvey et al., 2018b). Considering that there is no

definite conclusion on the focus question of whether HTP is harmful or not, we proposed a null hypothesis was that heated tobacco products were safe and non-toxic in the dose range tested when compared with traditional cigarettes.

In this paper, we use 3D biomimetic chip technology to systematically evaluate the toxicity of HTP and Cig. Specifically, we first analyzed and compared the differences between 2D and 3D model on cell culture, including cell growth status, characteristics and function maintenance. Then, the cell viability, morphological changes and apoptosis status of BEAS-2B cells treated by HTP and Cig were compared in detail. In the 3D culture state, BEAS-2B cells was stimulated by aqueous aerosol extracts (AqE) to produce inflammatory and anti-inflammatory factors, as well as the difference in the effects of linear damage and energy metabolism. The mechanism of BEAS-2B cells and mitochondrial damage caused by CSE was preliminarily discussed, so as to provide new ideas and evidences for the effective prevention of related diseases caused by tobacco products.

Materials and methods

Tobacco products and 3D Bio-mimetic chip

HTP for the preparation of AqE were purchased from the Korean market and produced by Hubei Tobacco Industry (Hubei, China). HTP includes an electronic heating device and a cigarette butt, called MOK and COO, respectively. In this study, one of tobacco sticks (same with THP COO ORIENTAL) was selected for this experiment (Wang et al., 2021). Cigarettes are derived from marketed in China (10 mg tar, 1 mg nicotine per cigarette) and have major chemical components that like to 3R4F (University of Kentucky).

The 3D Biomimetic Chip was purchased from Beijing Daxiang Biotech Co., Ltd. Each unit contains three wells, in which the wells on both sides are connected through the bottom, and the medium is added later to provide shear force and microgravity environment for the cultured cells through a certain swing during dynamic culture.

Cells grow at the bottom of the middle well of each unit, with a polydimethylsiloxane (PDMS) membrane at the bottom and modified by collagen I (Corning, USA).

Inoculation Culture of Cells on Chip

For the cell culture, human bronchial epithelium BEAS-2B cells were purchased from the American Type Culture Collection (ATCC; Manassas, VA, USA). Cells were resuscitated and cultured in DMEM complete medium (Corning, USA) supplemented with 10% fetal calf serum (FBS, Gibco, USA). The cells were incubated in a humidified atmosphere maintained at 37 ℃ and 5% CO_2. When the cells grew to about 80%, trypsin (Solarbio Technology, Beijing, China) digestion was used for routine subculture.

The inoculation of BEAS-2B cells on 3D chips was the same as that reported by Jing and Xiao et al (Jing et al., 2022; Xiao et al., 2022; Xiao et al., 2021). Briefly, the porous membrane was coated with type I collagen hydrogel (Corning, USA) in a carbon dioxide incubator (37.5 °C, 5 % CO_2) for 2 hours. After washing with sterile PBS, BEAS-2B cells were seeded on the microfluidic channel in the lower part of the left chamber and incubated in an inverted incubator at 37.5 °C for 2 h, so that the inoculated cells were attached to the surface of the porous membrane. Then, 100 μL medium was added to each chamber and the device was placed on an iBAC rocker (MR100110, Beijing Daxiang Biotechnology, China) for dynamic culture. With a swing angle of 30 degrees and a swing frequency of 1 circle / min, a relatively stable fluid flow rate and shear force can be achieved.

Preparation of AqE

According to the method of capturing carbonyl compounds (CORESTA Recommended Method No. 96; CORESTA Recommended Method No. 74), we connect two similar U-shaped traps in series. 40 mL of DMEM medium (excluding FBS and DMSO) are added into the front and rear tubes, respectively. Whole aerosols

from cigarettes (1 mg nicotine per cigarette) or HTP (0.6 mg nicotine per cigarette) were generated on a smoking machine (ESTONG, Qingdao, China) under the Health Canada Intense (HCI) machine puffing regime (55 mL puff taken over 2 s and repeated every 30 s). Considering the difference of nicotine content between Cig (0.1 mg/puff) and HTP (0.06 mg/puff), so we made sure the same volume of smoke extraction under the consistent suction mode (HCI) and puffs. AqEs were generated by bubbling 20×55 mL puffs from one Cig or HTP through 40 mL DMEM medium without added supplements or serum. After the preparation of Aqe (0.5 puffs/ml), the brown reagent bottle was sealed and stored in a refrigerator at 4 °C after sterilization with a 0.22 μM pinhole filter. According to the experimental requirements, 0.5 puffs/ml, 0.25 puffs/ml and 0.125 puffs/ml (**Supplementary Table 1 and 2**) were obtained by adding DMEM medium.

Cell Viability Detection

Cell viability between static culture (2D) and dynamic culture (3D) was determined by fluorescein diacetate (FDA, Sangon Biotech, China) fluorescence microplate method. Specifically, 5×10^3 cells / well were inoculated in a 3D chip and cultured continuously for 9 days. The culture medium in the culture plate was discarded when the cell viability was measured, and the cells were washed with sterile PBS solution. 100 μL FDA (10 μg/ml) was added and incubated at 37 °C for 30 min. Then the fluorescence intensity was measured by High Content Screening (HCS, PerkinElmer, USA) (excitation light: 485 nm, emission light: 538 nm).

Cell cytotoxicity, morphology and apoptosis

BEAS-2B cells were inoculated on a 3D chip at 1×10^4 cells/well with fresh medium. After 12 h, the cell medium was replaced with medium containing different concentrations of AqE (25 %, 50% and 100%). Viability of BEAS-2B cells was detected on 24 h after dosing according to instructions of CCK-8 assay kit (Solarbio

Technology, Beijing, China). The morphology and apoptosis (Nanjing Jiancheng Bioengineering, Jiangsu, China) of the cells were observed by inverted fluorescence microscope.

Enzyme-linked immunosorbent assay (ELISA)

The expression of inflammatory factors in BEAS-2B cells was detected by enzyme-linked immunosorbent assay. Briefly, 1.5×10^4 cells/well were seeded on a 3D chip, and different doses of AqE (Both Cig and HTP) replaced completely medium (DMEM with 10% FBS) after 24 h of inoculation. The cells were cultured in two different ways, 3D dynamic culture and 2D static culture. The supernatant of cells treated with different concentrations of AqE was collected after 24 h of treatment, and the levels of IL-6/8/1β, TNF-α, LDH, SOD, MDA and GSH/GSSG were determined by ELISA kit (Shanghai Enzyme-linked Biotechnology, Shanghai, China). The specific operation method was carried out according to the instructions of the corresponding kits.

Determination of ATP, reactive oxygen species (ROS) and mitochondrial membrane potential

As described above, the number of cells inoculated and the time of dosing were consistent with ELISA experiments. After 24 h of treatment with different AqE, cells were collected and lysised, then ATP content was determined according to the instructions of ATP kit (Solarbio Technology, Beijing, China). For determining ROS and mitochondrial membrane potential, cells were incubated with ROS reagent (Beyotime Biotechnology, Beijing, China) or membrane potential detection reagent (Yeasen Biotechnology, Shanghai, China) for 20 min. Finally, the excess fluorescent dyes were washed off, and cells was detected with HCS. The detailed protocol for using HCS are performed as described previously (Gonzalez-Suarez et al., 2016; Wang et al., 2021).

Real-time fluorescence quantitative PCR

Total RNA was extracted using the Trizol reagent (Solarbio Technology, Beijing, China). The reverse transcription reaction system was configured according to the kit instructions (Takara, Japan). qPCR was performed using SYBR Premix Ex Taq (Takara, Japan). The primer sequences used in this study are listed in Table 1. Using the $2^{-\Delta\Delta ct}$ method to calculate the relative expression of each target gene.

Table 1 Primer sequences used for RT-PCR analysis.

mRNA	Sequences (5'–3')	Product (bp)
GAPDH	Fw: GTTGCAACCGGGAAGGAAAT Rv: AGTTAAAAGCAGCCCTGGTG	214
CS	Fw: CGACCCTTACCTGTCCTTTG Rv: CTCGCTGACAGGTATTATCGC	236
IDH2	Fw: TTTTGCAACGCCATAGGACT Rv: CGGGTCATCTCATGACCATC	109
OGDH	Fw: AGCTGAGCCGCAAGACAG Rv: CAGCCAAGCTCAGTACATCT	242

Statistics

All data were analyzed by SPSS 24.0 software and all experiments were repeated at least three times. Values are expressed as $\bar{X} \pm SD$. The differences between the two groups were compared by independent sample *t*-test. One-way ANOVA was used for comparison between multiple groups, and LSD test was used for further comparison. $p < 0.05$ indicated that the difference was statistically significant.

Results

Aerosol generation regimens and AqE nicotine quantification

Suppl Table 1 and 2 showed the preparation method of smoke extract and the content of nicotine in total extract. As described in the experimental method, 20 puffs of smoke were poured into 40 mL culture medium (DMEM) to prepare AqE. The total content of nicotine in the extract of HTP and ig was 17.48 ± 1.34 and 26.32 ± 2.26 μg, respectively. With the same number of puffs, the nicotine content of cigarettes was 1.5

times higher than that of HTP.

Difference on cell proliferation and activity retention between 2D and 3D culture

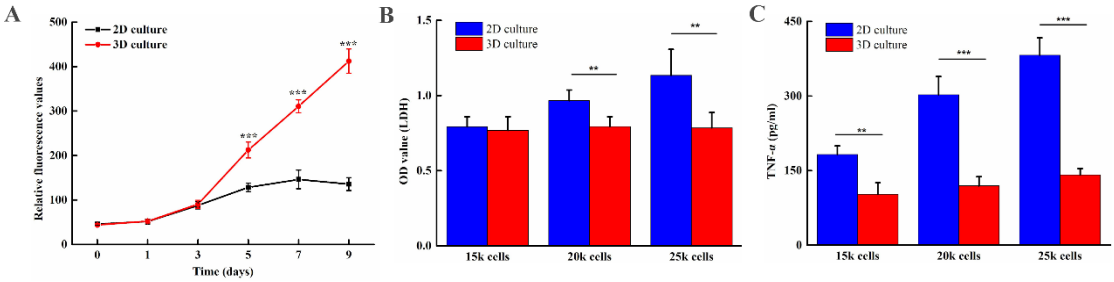

Figure 1. Growth curves, toxicity sensitivity and growth status of the 2D and 3D models. (A) Cell viability was indicated by luminescence intensity measured using fluorescein diacetate fluorescence microplate method. (B) Cell growth state was represented by the content of LDH and TNF-α in the cell culture medium when BEAS-2B cells were cultured on the 2D or 3D models and seeded different densities. All data are presented as means ± SD of three replicates.

We compared the differences in proliferation rate and growth status between 2D and 3D cell culture. The results are shown in Figure 1. The same cell density (5×10^3 cells / well) was inoculated and cultured in different ways (2D or 3D), the total number of cells was counted by relative fluorescence value. The results showed that there was no significant difference in the proliferation rate of cells in the first 3 days (**Fig. 1A**), while a significant difference ($p < 0.001$) was observed on 5th day. Meanwhile, the results showed that with the increasing of growth time, the cells cultured in 3D way were still rapidly proliferating (even more than 9 days), while the cells cultured in 2D showed signs of proliferation reaching the plateau phase at 7 days. We observed the growth status of cells with different cell densities in 2D and 3D way, and the results were shown in Figure 1B and C. The cell growth state was represented by the content of LDH and tumor necrosis factor TNF-α in the supernatant of culture medium, which marked the change of cell membrane permeability and the degree of cell stimulation, respectively. The results showed that with the increasing of cell concentrations, the contents of LDH and TNF-α gradually increased, and changes of 2D culture was significantly more than the of 3D culture ($p < 0.01$), which confirmed

that the damage of cell membrane and the stimulation (inflammation) in 2D culture were much greater than those in 3D culture.

Effects of HTP and Cig on cell viability, morphology and apoptosis

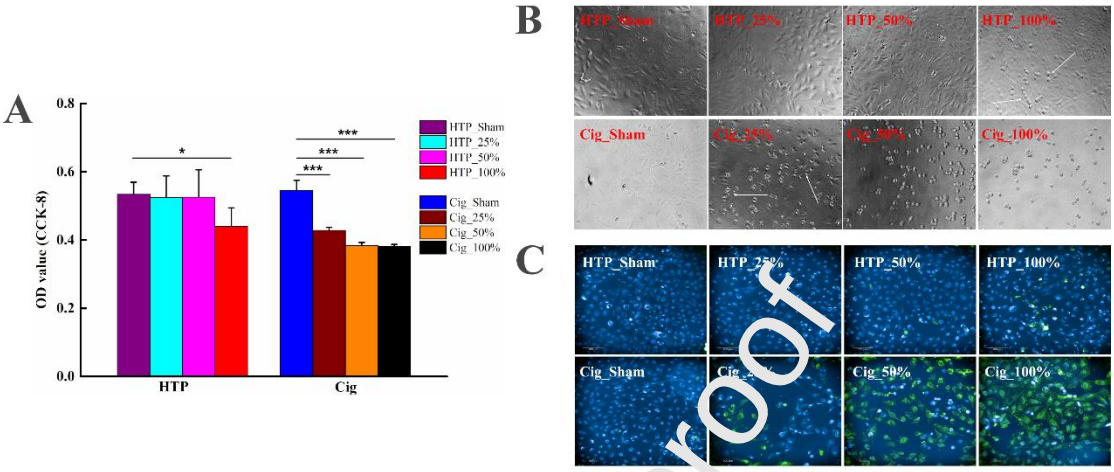

Figure 2. (A) Cytotoxicity measured by CCK-8 assay using BEAS-2B cells based on 3D Biomimetic Chip. Data are presented as mean ± SD, N = 3, for all tests. (B) The morphological changes of BEAS-2B cells treated with AqE (HTP or Cig) were observed by optical microscope (100×), and the white arrow indicated that the cells became oval. (C) The apoptosis of BEAS-2B cells was observed by fluorescence microscopy (Annexin V-FITC and DAPI assay, Annexin V-FITC is green fluorescence and DAPI blue). Green fluorescence indicated that the cells with loss of cell membrane integrity were in a necrotic state (Scale bar: 100 μm). HTP_Sham means control group of HTP, identical to Cig_Sham.

The effects of HTP or Cig on the proliferation of BEAS-2B were shown in Figure 2A. It's easy to observe that the proliferation abilities of treatment groups were significantly lower than that of control group ($p < 0.001$), while significant reduction of proliferation ability were only found in the HTP_100% group compared with control group. Meanwhile, the results showed that HTP_100 % and Cig_25 % were similar in the effects on the proliferation of BEAS-2B cells. The effects of AqE (HTP or Cig) on cell morphology was shown in Fig 2B. It can be clearly observed that the normal cell growth state was flat or fusiform, and the cytoplasm was abundant. After treated with AqE, it can be found that the cells were observed to become spherical in HTP_100 % group and Cig groups (Cig_10, Cig_23 and Cig_50). The experimental results of apoptosis (**Fig. 2C**, green fluorescence indicates apoptosis or necrosis of cells) were consistent with the observation of cell morphology (**Fig. 2B**). Obvious

apoptosis and necrosis of BEAS-2B cells were observed in HTP_100 % group and Cig groups, and the apoptosis state of Cig group was more obvious with the increasing of smoke extract concentration.

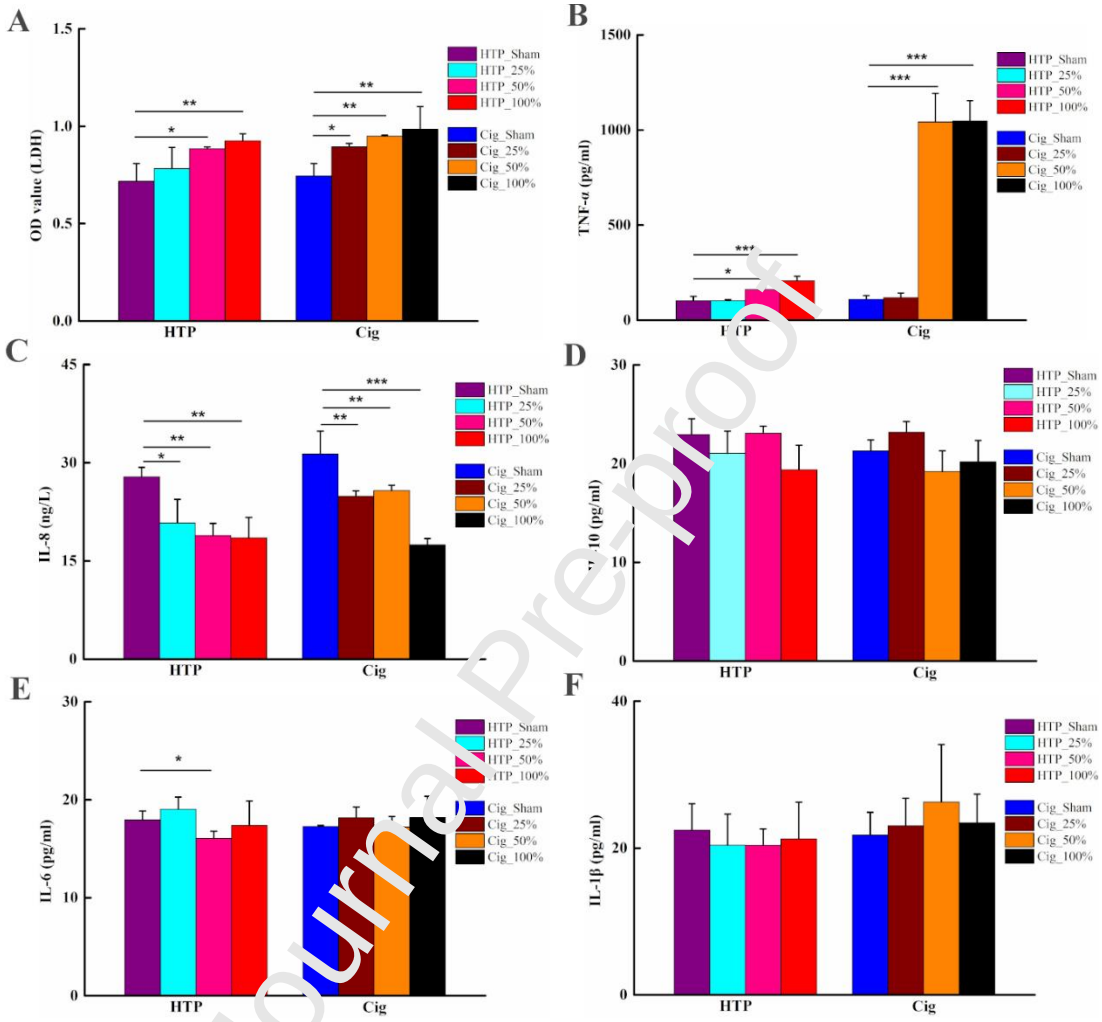

Figure 3. Quantification of cytokine in BEAS-2B cells treated with AqE from either HTP and Cig. Protein levels of (A) LDH, (B) TNF-α, (C) IL-8, (D) IL-6, (E) IL-10 and (F) IL-1β. * means $p < 0.05$, ** $p < 0.01$, ***$p < 0.001$, as compared with the negative control (one-way ANOVA test). Bars represent mean ± SD of biological replicates (n=3).

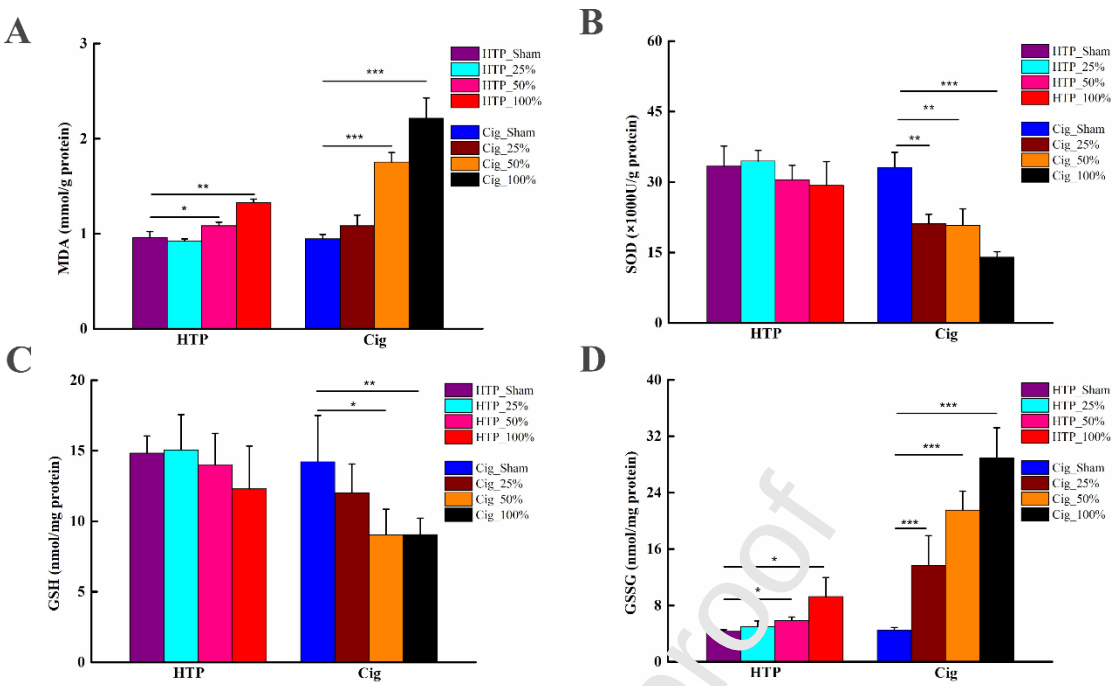

Figure 4. The effects of AqE (HTP or Cig) on cytokine release from BEAS-2B cells cultured in 3D chip model. (A) MDA, (B) SOD, (C)GSH, (D) GSSG. *, **, ***, significant difference compared to untreated cells where $p<0.05$, $p<0.01$ and $p<0.001$, respectively.

ELISA was used to detect the cytokines release in BEAS-2B cells after AqE treatment, and the experimental results were shown in Figures 3 and 4. The experimental results (**Fig. 3A**) showed that the LDH content increased significantly with the increasing of AqE (HTP and Cig) concentration and there was a significant difference when compared with control group ($p<0.05$). Meanwhile, the results confirmed that the cell membrane permeability of Cig groups was much higher than that of HTP groups. The same experimental results were shown in the expression of inflammatory factors such as TNF-α (**Fig. 3B**) and IL-8 (**Fig. 3C**). The level of inflammatory factors in the cell supernatant was concentration-dependent with the concentration of AqE stimulation, and there was a significant difference between the experimental groups and control group. However, there was no differences in the expression of IL-6, IL-10 and IL-1β inflammatory factors (**Fig. 3D, E and F**). Here we used conventional indicators of oxidative stress (SOD, GSH and GSSG) and lipid peroxidation (MDA) to examine AqE-induced oxidative stress in BEAS-2B cells. The results (**Fig. 4**) showed that after AqE treatment for 24 hours, the oxidative stress indicators of the Cig groups showed a significant decrease (SOD and GSH/GSSG) in

a dose-dependent manner ($p<0.05$), while the HTP groups showed an upward trend of GSSG only in the HTP_100% group. The above results showed that SOD and GSH were significantly consumed in the Cig groups, reflecting the destruction of cell redox balance. Similarly, the lipid peroxidation index MDA was found increasing in a concentration-dependent manner.

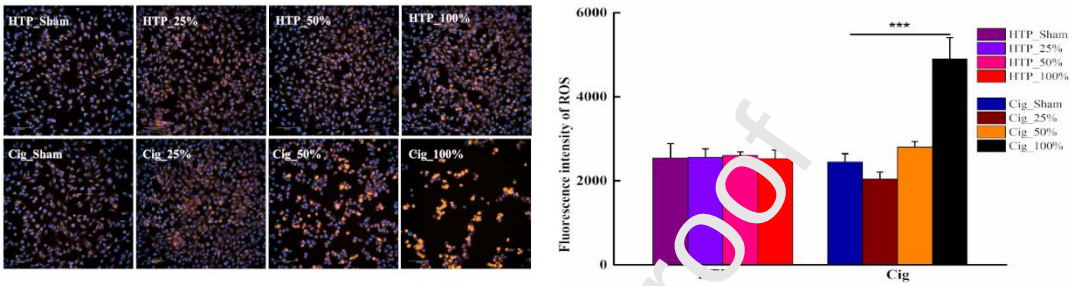

Figure 5. The intensity of orange fluorescence was positively correlated with the content of ROS in BEAS-2B cells treated with AqE (ROS assay, DAPI regent for nucleus. Scale bar: 100 μm). Conditions were performed in triplicate with the mean value plotted as a bar and error bars representing standard error of the mean. Data were analyzed using an ordinary one-way ANOVA, *** means $p < 0.001$.

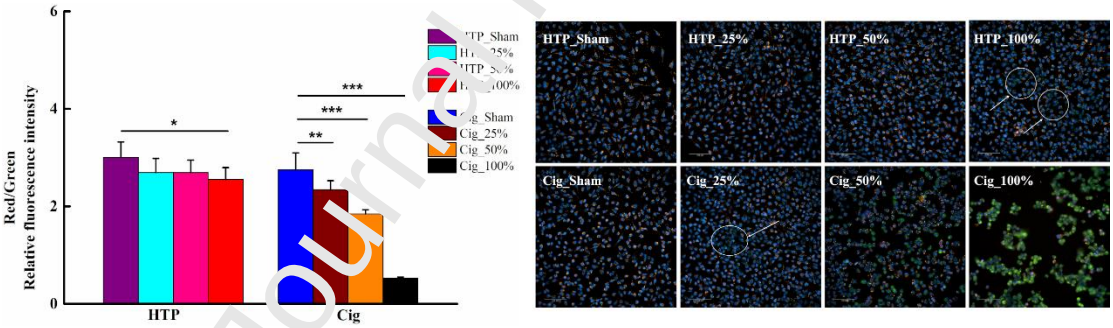

Figure 6. Fluorescence microscope (High Content Screening) assessment of mitochondrial membrane potential after AqE-treated (JC-1 assay, DAPI regent for nucleus. Scale bar: 100 μm). Red fluorescence indicated the normal mitochondria, and green fluorescence reflects the decrease and loss of membrane potential. The right histogram was a quantitative analysis of the image results, which was measured by the ratio of red and green fluorescence intensity. Data were analyzed using an ordinary one-way ANOVA and horizontal brackets denote comparisons between conditions that are statistically significant (p-value < 0.05, 0.01 or 0.001).

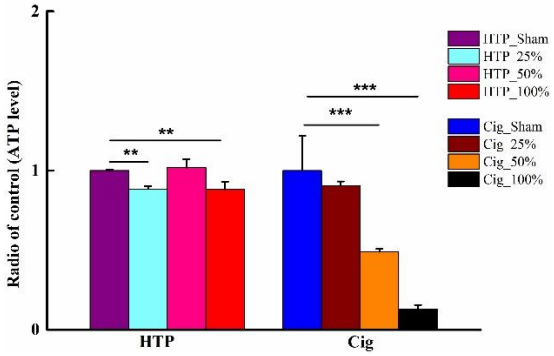

Figure 7. Relative ATP levels in BEAS-2B cells after the 24 h of treatment with AqE (HTP or Cig). All data presented the mean ± SD (n=3), * denotes *p*-value < 0.05, ** denotes *p* -value < 0.01 and *** denotes *p* -value < 0.001.

According to Figure 5, the intracellular ROS content of BEAS-2B cells was changed after exposure to AqE, which could be distinguished by the intensity of orange fluorescence. The results showed that the difference between Cig_100 % group and Sham group was extremely significant ($p < 0.001$), but no significant difference was observed in all of HTP groups. The effects of AqE on mitochondrial membrane potential after 24 hours was shown in figure 6. The results showed that HTP_100 % affected the mitochondrial membrane potential (the cells in the white circle were unhealthy cells) and there was a significant difference compared with the control group ($p < 0.05$). At the same time, the results showed that AqE (Cig) had a more obvious effects on the mitochondrial membrane potential of BEAS-2B cells and showed a dose-dependent effect. The amount of ATP produced by cells proved the effects of AqE on BEAS-2B cells (**Fig.7**). Consistent with the results of the effects of AqE on mitochondrial membrane potential, Cig_25 % AqE could significantly affect ATP production ($p < 0.01$), while HTP only significantly inhibited ATP production at HTP_100 %.

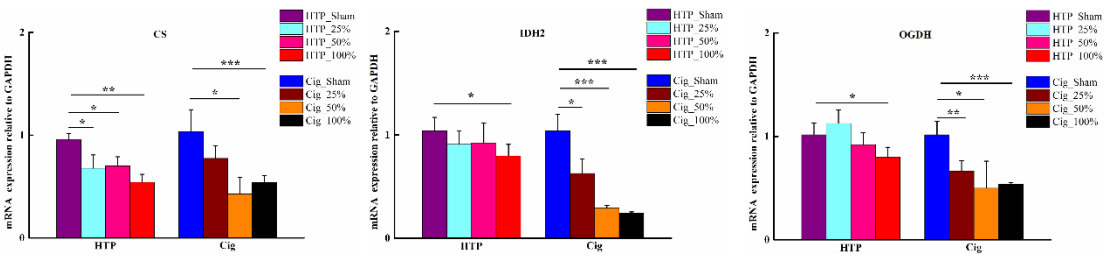

Figure 8. AqE induced the inflammation reaction and mitochondrial damage in BEAS-2B cells, leading to down-regulation of key rate-limiting enzyme genes (CS, IDH2 and OGDH) in the tricarboxylic acid cycle. Data were shown as the means ± SD. One-way ANOVA was used to

compare the differences, *$p < 0.05$, **$p < 0.01$ and ***$p < 0.001$ compared to the Sham group. CS, Citrate Synthase. IDH2, Isocitrate Dehydrogenase. OGDH, α-ketoglutarate Dehydrogenase.

The effects of AqE on the mRNA expression of TCA (tricarboxylic acid cycle)-related key enzyme in BEAS-2B cells were shown in Figure 8. Compared with Sham group, HTP_100% significantly down-regulated IDH2 and OGDH genes, while for CS gene, mRNA the expressions were down-regulated in all of HTP experimental groups, and showed a dose-dependent effect. Meanwhile, the experimental results showed that all genes (CS, IDH2 and OGDH) in all Cig groups were significantly down-regulated when compared with Sham group ($p < 0.01$) and showed a significant concentration gradient effect.

Discussion

In this paper, we used a novel 3D biomimetic chip model to evaluate the potential toxicity of HTP, which provided a 3D microenvironment and fluid shear force for the growth of BEAS-2B cells. Before the formal evaluation of HTP, we explored the difference between 3D and 2D culture (**Fig. 1**). The results showed that the proliferation ability (**Fig. 1A**) and growth status of dynamically cultured cells (3D) were significantly improved (**Fig. 1B**, less harmful cytokine release of LDH and TNF-α), which was consistent with other reported literatures (Jing et al., 2022; Xiao et al., 2022). This indicates that BEAS-2B cells have similar functions to tissues in the case of chip model dynamic culture (3D), so that nutrients and oxygen can be transferred to the deep cells in time, which is convenient for cells to absorb nutrients to meet the proliferation needs. Meanwhile, the microgravity environment provided by 3D simulates the physiological growth state of cells to ensure the characteristics and vitality of cells (Bahmaee et al., 2020; Wang et al., 2020).

The 3D chip model was used to evaluate the toxic effects of AqE (HTP and Cig) on BEAS-2B cells in terms of proliferation ability, morphological changes, induction of apoptosis and cytokine release. The experimental results were shown in Figure 2-4. The increase of AqE concentration seriously affected the cell proliferation ability, but this result was only significantly different in Cig and showed a dose-dependent effect

(Hoshino et al., 2001; Hou et al., 2020; Romagna et al., 2013), and only in the HTP_100 % group. The morphological changes (shrinkage and ovalization) and apoptosis/necrosis of BEAS-2B cells were related to the dose of AqE, which showed that the cells emitted strong green fluorescence at high concentrations (Annexin V-FITC assay). Pulmonary exposure to inhaled smoke or other harmful components is often associated with inflammation, which is involved in host defense, systemic response and repair. There is a large body of data showing that airway epithelial cell exposure to cigarette smoke leads to the release of a complex mixture of inflammatory mediators (Alexander et al., 2015; Heijink et al., 2013; Herr et al., 2020; Rastrick et al., 2013). According to the release of cytokines, BEAS-2B cells were subjected to obvious oxidative stress at different concentrations of Cig, corresponding to the up-regulation of inflammation-related factors (LDH, TNF-α and IL-8), that's consistent with the published literatures (Anthérieu et al., 2017; Bengalli et al., 2017; Cervellati et al., 2014; Ganguly et al., 2020; Herr et al., 2020; Higham et al., 2018; Higham et al., 2016; Leslie et al., 2017). However, HTP only showed a certain inflammatory state at high doses. As far as I know, this is the first time to evaluate the potential hazards of HTP under 2D and 3D culture techniques. The above results indicated that the substances other than nicotine were more likely to cause obvious oxidative stress and even cell necrosis, which was consistent with the reported literature (Gasparyan et al., 2018; Mallock et al., 2018).

Studies have shown that cigarette smoke can cause oxidative stress and inflammatory response (Kamp et al., 2011; Prakash et al., 2017; Prasad et al., 2017) in a variety of cell lines, resulting in cell damage, and thus causing a variety of cell death, including apoptosis (Mizumura et al., 2014; Prakash et al., 2017), necrosis (Vayssier-Taussat et al., 2001; Vayssier et al., 1998), pyroptosis (Kong et al., 2022; Zhang et al., 2021; Zhao et al., 2021)and ferroptosis (Liu et al., 2022; Tang et al., 2021). At the subcellular level, although there is a lack of systematic research, single organelle damage, such as mitochondrial structural dysfunction, has been reported in the literature (Decker et al., 2021; Giordano et al., 2022; Li et al., 2022). Mitochondria are not only the factory of energy production in cells, but also the important signal

transduction center in the body. Mitochondria participate in the regulation of the whole growth activity of cells by regulating the production and consumption of reactive oxygen species and the intensity of Ca ion signal, so as to communicate and feedback the related signals with the nucleus. Mitochondria are organelles that are very sensitive to external toxicants and oxidative damage. Many studies have reported that smoke causes mitochondrial damage (Cloonan et al., 2016; Maremanda et al., 2019; Wang et al., 2019; Wang et al., 2020). As shown in Figure 5-6, when the toxic substances of AqE (aldehydes and phenols, etc.) enter the cells, the production of reactive oxygen species (ROS) increases (**Fig. 5**), and ROS free radicals can cause oxidative stress damage to mitochondrial membrane, mitochondrial DNA (mtDNA) and mitochondrial enzymes. When excessive reactive oxygen species are generated in mitochondria, it will also cause peroxidation of the mitochondrial membrane, resulting in different degrees of damage to the mitochondrial membrane structure (Cloonan et al., 2016; Maremanda et al., 2019), which will lead to an increase in the permeability of the mitochondrial membrane, and destroy the proton gradient inside and outside the mitochondrial membrane that was originally in a stable state. The stable mitochondrial membrane potential formed by these proton gradients will gradually decrease with the destruction of the proton gradient, showing that the ratio of red / green fluorescence intensity of the mitochondrial membrane potential continues to decrease (**Fig. 6**). Mitochondria are the most important place to produce energy (ATP). Due to the oxidative stress caused by ROS and the change of membrane potential, the structure and function of mitochondria are destroyed, which seriously affects the production of ATP energy (**Fig. 7**). In summary, under the action of external factors, the increase of intracellular ROS content leads to oxidative stress and inflammation of cells, while the breakdown of cell homeostasis leads to more ROS production. Due to the enhanced permeability of the cell membrane, external small molecule compounds enter the cell and act on subcellular organelles (endoplasmic reticulum, mitochondria, etc.), causing intracellular structure to be destroyed and eventually causing apoptosis and necrosis of cells.

Meanwhile, it is well known that mitochondria play an important role in energy

metabolism because they are important carriers in the TCA cycle. (Alcázar-Fabra et al., 2016; Brun and Maechler, 2016; Garabadu et al., 2019; Gray et al., 2014; Iacobazzi and Infantino, 2014; Pearce et al., 2013). The above results have found that AqE (especially for Cig) affects the structure and function of mitochondria (Aydın et al., 2022; Datta et al., 2019). Here, the effects of AqE on the key rate-limiting enzymes (CS, IDH2 and ODGH) in TCA were specifically discussed. The results showed that the mitochondrial dysfunction caused by AqE resulted in the down-regulation of related enzyme gene expression, and the effect of Cig on was greater than that of HTP.

Conclusion

In this study, 3D chip model was used to culture BEAS-2B cells, which can better simulate the microenvironment of cell growth and maintain cell characteristics. After AqE treatment, the toxicity of HTP and Cig was evaluated by cell proliferation assay, apoptosis, cytokine release, mitochondrial-related oxidative stress and TCA rate-limiting enzyme gene regulation. Compared with Cig, HTP had a weaker toxic effect on BEAS-2B cells even at HTP_100%, mainly manifested in limited inhibition of cell proliferation, only a small amount of apoptosis, necrosis, and inflammatory response, minor impairment of mitochondrial structure and relatively low impact on gene expression of key enzymes in the TCA cycle. Oxidative stress and mitochondrial dysfunction are mutually causal, and the interaction between them eventually leads to apoptosis and necrosis. Although toxicity of HTP is lower than that of Cig, HTP is not absolutely no-harm and real safe based on 3D chip model, so the security risks of HTP should be taken seriously and regulated accordingly.

3D models of organ chips and lung organoids are at the forefront of the toxicological studies. In the foreseeable future, they would be very likely to replace animals and cell culture to study the mechanism of tobacco products acting on target organs. The high-throughput and sensitive specificity of organ chips can meet the needs of studying the weak biological effects of HTP, the potential toxicology of HTP can be better explored at the molecular level based on its findings. However, we should also pay attention to the limitations of 3D models. It is well known that the

existing 3D models often consist of two types of cells, and a small number of models contain three or four different types of cells, which is not enough to comprehensively evaluate the smoke of thousands of compounds.

Disclosure statement

The authors declare that they have no known competing financial interests or personal relationships that could have appeared to influence the work reported in this paper.

Funding

This work was supported by the Provincial and Ministerial Major Project of China (grant numbers 2019420000340623,11020200[illegible]006 (XX-02)).

References

Alcázar-Fabra, M., Navas, P., and Brea-Calvo, G. (2016). Coenzyme Q biosynthesis and its role in the respiratory chain structure. *Biochim Biophys Acta* **1857**, 1073-1078.

Alexander, J. J., Chaves, L. D., Chang, A., Jacob, A., Ritchie, M., and Quigg, R. J. (2015). CD11b is protective in complement-mediated immune complex glomerulonephritis. *Kidney Int* **87**, 930-9.

Anthérieu, S., Garat, A., Beauval, N., Soyez, M., Allorge, D., Garçon, G., and Lo-Guidice, J. M. (2017). Comparison of cellular and transcriptomic effects between electronic cigarette vapor and cigarette smoke in human bronchial epithelial cells. *Toxicol In Vitro* **45**, 417-425.

Aydın, B., Oğuz, A., Şekeroğlu, V., and Atlı Şekeroğlu, Z. (2022). Whey protein protects liver mitochondrial function against oxidative stress in rats exposed to acrolein. *Arh Hig Rada Toksikol* **73**, 200-206.

Başaran, R., Güven, N. M., and Eke, B. C. (2019). An Overview of iQOS(®) as a New Heat-Not-Burn Tobacco Product and Its Potential Effects on Human Health and the Environment. *Turk J Pharm Sci* **16**, 371-374.

Bengalli, R., Ferri, E., Labra, M., and Mantecca, P. (2017). Lung Toxicity of Condensed Aerosol from E-CIG Liquids: Influence of the Flavor and the In Vitro Model Used. *Int J Environ Res Public Health* **14**.

Berkowitz, L., Schultz, B. M., Salazar, G. A., Pardo-Roa, C., Sebastián, V. P., Álvarez-Lobos, M. M., and Bueno, S. M. (2018). Impact of Cigarette Smoking on the Gastrointestinal Tract Inflammation: Opposing Effects in Crohn's Disease and Ulcerative Colitis. *Front Immunol* **9**, 74.

Brun, T., and Maechler, P. (2016). Beta-cell mitochondrial carriers and the diabetogenic stress response. *Biochim Biophys Acta* **1863**, 2540-9.

Carnevali, S., Petruzzelli, S., Longoni, B., Vanacore, R., Barale, R., Cipollini, M., Scatena, F., Paggiaro, P., Celi, A., and Giuntini, C. (2003). Cigarette smoke extract induces oxidative stress and apoptosis in human lung fibroblasts. *Am J Physiol Lung Cell Mol Physiol* **284**, L955-63.

Cervellati, F., Muresan, X. M., Sticozzi, C., Gambari, R., Montagner, G., Forman, H. J., Torricelli, C., Maioli, E., and Valacchi, G. (2014). Comparative effects between electronic and cigarette smoke in human keratinocytes and epithelial lung cells. *Toxicol In Vitro* **28**, 999-1005.

Cloonan, S. M., Glass, K., Laucho-Contreras, M. E., Bhashyam, A. R., Cervo, M., Pabón, M. A., Konrad, C., Polverino, F., Siempos, II, Perez, E., Mizumura, K., Ghosh, M. C., Parameswaran, H., Williams, N. C., Rooney, K. T., Chen, Z. H., Goldklang, M. P., Yuan, G. C., Moore, S. C., Demeo, D. L., Rouault, T. A., D'Armiento, J. M., Schon, E. A., Manfredi, G., Quackenbush, J., Mahmood, A., Silverman, E. K., Owen, C. A., and Choi, A. M. (2016). Mitochondrial iron chelation ameliorates cigarette smoke-induced bronchitis and emphysema in mice. *Nat Med* **22**, 163-74.

CORESTA Recommended Method No. 96. Determination of formaldehyde and acetaldehyde in e-vapour product aerosol [S]. 2021.

CORESTA Recommended Method No. 74. Determination of Selected Carbonyls in Mainstream Cigarette Smoke by HPLC [S]. 2014.

Cukierman, E., Pankov, R., Stevens, D. R., and Yamada, K. M. (2001). Taking cell-matrix adhesions to the third dimension. *Science* **294**, 1708-12.

Datta, K. K., Patil, S., Patel, K., Babu, N., Raja, R., Nanjappa, V., Mangalaparthi, K. K., Dhaka, B., Rajagopalan, P., Deolankar, S. C., Kannan, R., Kumar, P., Prasad, T. S. K., Mathur, P. P., Kumari, A., Manoharan, M., Coral, K., Murugan, S., Sidransky, D., Gupta, R., Gupta, R., Khanna-Gupta, A., Chatterjee, A., and Gowda, H. (2019). Chronic Exposure to Chewing Tobacco Induces Metabolic Reprogramming and Cancer Stem Cell-Like Properties in Esophageal Epithelial Cells. *Cells* **8**.

Decker, S. T., Kwon, O. S., Zhao, J., Hoidal, J. R., Heuckstadt, T., Richardson, R. S., Sanders, K. A., and Layec, G. (2021). Skeletal muscle mitochondrial adaptations induced by long-term cigarette smoke exposure. *Am J Physiol Endocrinol Metab* **321**, E80-e89.

Doke, S. K., and Dhawale, S. C. (2015). Alternatives to animal testing: A review. *Saudi Pharm J* **23**, 223-9.

Fricker, M., Goggins, B. J., Mateer, S., Jones, B., Kim, R. Y., Gellatly, S. L., Jarnicki, A. G., Powell, N., Oliver, B. G., Radford-Smith, G., Talley, N. J., Walker, M. M., Keely, S., and Hansbro, P. M. (2018). Chronic cigarette smoke exposure induces systemic hypoxia that drives intestinal dysfunction. *JCI Insight* **3**.

Ganguly, K., Nordström, A., Thimraj, T. A., Rahman, M., Ramström, M., Sompa, S. I., Lin, E. Z., O'Brien, F., Koelmel, J., Ernstgård, L., Johanson, G., Pollitt, K. J. G., Palmberg, L., and Upadhyay, S. (2020). Addressing the challenges of E-cigarette safety profiling by assessment of pulmonary toxicological response in bronchial and alveolar mucosa models. *Sci Rep* **10**, 20460.

Garabadu, D., Agrawal, N., Sharma, A., and Sharma, S. (2019). Mitochondrial metabolism: a common link between neuroinflammation and neurodegeneration. *Behav Pharmacol* **30**, 642-652.

Gasparyan, H., Mariner, D., Wright, C., Nicol, J., Murphy, J., Liu, C., and Proctor, C. (2018). Accurate measurement of main aerosol constituents from heated tobacco products (HTPs): Implications for a fundamentally different aerosol. *Regul Toxicol Pharmacol* **99**, 131-141.

Giordano, L., Gregory, A. D., Pérez Verdaguer, M., Ware, S. A., Harvey, H., DeVallance, E., Brzoska, T., Sundd, P., Zhang, Y., Sciurba, F. C., Shapiro, S. D., and Kaufman, B. A. (2022). Extracellular Release of Mitochondrial DNA: Triggered by Cigarette Smoke and Detected in

COPD. *Cells* **11**.

Gonzalez-Suarez, I., Martin, F., Marescotti, D., Guedj, E., Acali, S., Johne, S., Dulize, R., Baumer, K., Peric, D., Goedertier, D., Frentzel, S., Ivanov, N. V., Mathis, C., Hoeng, J., and Peitsch, M. C. (2016). In Vitro Systems Toxicology Assessment of a Candidate Modified Risk Tobacco Product Shows Reduced Toxicity Compared to That of a Conventional Cigarette. *Chem Res Toxicol* **29**, 3-18.

Gray, L. R., Tompkins, S. C., and Taylor, E. B. (2014). Regulation of pyruvate metabolism and human disease. *Cell Mol Life Sci* **71**, 2577-604.

Heijink, I. H., de Bruin, H. G., van den Berge, M., Bennink, L. J., Brandenburg, S. M., Gosens, R., van Oosterhout, A. J., and Postma, D. S. (2013). Role of aberrant WNT signalling in the airway epithelial response to cigarette smoke in chronic obstructive pulmonary disease. *Thorax* **68**, 709-16.

Herr, C., Tsitouras, K., Niederstraßer, J., Backes, C., Beisswenger, C., Dong, L., Guillot, L., Keller, A., and Bals, R. (2020). Cigarette smoke and electronic cigarettes differentially activate bronchial epithelial cells. *Respir Res* **21**, 67.

Higham, A., Bostock, D., Booth, G., Dungwa, J. V., and Singh, D. (2018). The effect of electronic cigarette and tobacco smoke exposure on COPD bronchial epithelial cell inflammatory responses. *Int J Chron Obstruct Pulmon Dis* **13**, 989-1000.

Higham, A., Rattray, N. J., Dewhurst, J. A., Trivedi, D. K., Fowler, S. J., Goodacre, R., and Singh, D. (2016). Electronic cigarette exposure triggers neutrophil inflammatory responses. *Respir Res* **17**, 56.

Hoshino, Y., Mio, T., Nagai, S., Miki, H., Ito, J., and Izumi, T. (2001). Cytotoxic effects of cigarette smoke extract on an alveolar type II cell-derived cell line. *Am J Physiol Lung Cell Mol Physiol* **281**, L509-16.

Hou, W., Hu, S., Yong, K.-t., Zhang, Y., and Ma, H. (2020). Cigarette smoke-induced malignant transformation via STAT3 signaling in pulmonary epithelial cells in a lung-on-a-chip model. *Bio-Design and Manufacturing* **3**, 383-395.

Iacobazzi, V., and Infantino, V. (2014). Citrate--new functions for an old metabolite. *Biol Chem* **395**, 387-99.

Jing, B., Yan, L., Li, J., Luo, P., Ai, X., and Tu, P. (2022). Functional Evaluation and Nephrotoxicity Assessment of Human Renal Proximal Tubule Cells on a Chip. *Biosensors (Basel)* **12**.

Kamp, D. W., Shacter, E., and Weitzman, S. A. (2011). Chronic inflammation and cancer: the role of the mitochondria. *Oncology (Williston Park)* **25**, 400-10, 413.

Kennedy-Feitosa, E., Cattani-Cavalieri, I., Barroso, M. V., Romana-Souza, B., Brito-Gitirana, L., and Valenca, S. S. (2019). Eucalyptol promotes lung repair in mice following cigarette smoke-induced emphysema. *Phytomedicine* **55**, 70-79.

Kong, X., Gao, M., Liu, Y., Zhang, P., Li, M., Ma, P., Shang, P., Wang, W., Liu, H., Zhang, Q., and Feng, F. (2022). GSDMD-miR-223-NLRP3 axis involved in B(a)P-induced inflammatory injury of alveolar epithelial cells. *Ecotoxicol Environ Saf* **232**, 113286.

Leslie, L. J., Vasanthi Bathrinarayanan, P., Jackson, P., Mabiala Ma Muanda, J. A., Pallett, R., Stillman, C. J. P., and Marshall, L. J. (2017). A comparative study of electronic cigarette vapor extracts on airway-related cell lines in vitro. *Inhal Toxicol* **29**, 126-136.

Li, L., Liu, Y., Liu, X., Zheng, N., Gu, Y., Song, Y., and Wang, X. (2022). Regulatory roles of external cholesterol in human airway epithelial mitochondrial function through STARD3 signalling.

Clin Transl Med **12**, e902.

Liu, J., Zhang, Z., Yang, Y., Di, T., Wu, Y., and Bian, T. (2022). NCOA4-Mediated Ferroptosis in Bronchial Epithelial Cells Promotes Macrophage M2 Polarization in COPD Emphysema. *Int J Chron Obstruct Pulmon Dis* **17**, 667-681.

Mallock, N., Böss, L., Burk, R., Danziger, M., Welsch, T., Hahn, H., Trieu, H. L., Hahn, J., Pieper, E., Henkler-Stephani, F., Hutzler, C., and Luch, A. (2018). Levels of selected analytes in the emissions of "heat not burn" tobacco products that are relevant to assess human health risks. *Arch Toxicol* **92**, 2145-2149.

Maremanda, K. P., Sundar, I. K., and Rahman, I. (2019). Protective role of mesenchymal stem cells and mesenchymal stem cell-derived exosomes in cigarette smoke-induced mitochondrial dysfunction in mice. *Toxicol Appl Pharmacol* **385**, 114788.

Marinucci, L., Coniglio, M., Valenti, C., Massari, S., Di Michele, A., Billi, M., Bruscoli, S., Negri, P., Lombardo, G., Cianetti, S., and Pagano, S. (2022). In Vitro effects of alternative smoking devices on oral cells: Electronic cigarette and heated tobacco product versus tobacco smoke. *Arch Oral Biol* **144**, 105550.

Mazzoleni, G., Di Lorenzo, D., and Steimberg, N. (2009). Modelling tissues in 3D: the next future of pharmaco-toxicology and food research? *Genes Nutr* **4**, 13-22.

McKelvey, K., Popova, L., Kim, M., Chaffee, B. W., Vijayaraghavan, M., Ling, P., and Halpern-Felsher, B. (2018a). Heated tobacco products likely appeal to adolescents and young adults. *Tob Control* **27**, s41-s47.

McKelvey, K., Popova, L., Kim, M., Lempert, L. K., Chaffee, B. W., Vijayaraghavan, M., Ling, P., and Halpern-Felsher, B. (2018b). IQOS labelling will mislead consumers. *Tob Control* **27**, s48-s54.

Mio, T., Romberger, D. J., Thompson, A. B., Robbins, R. A., Heires, A., and Rennard, S. I. (1997). Cigarette smoke induces interleukin-8 release from human bronchial epithelial cells. *Am J Respir Crit Care Med* **155**, 1770-6.

Mizumura, K., Cloonan, S. M., Nakahira, K., Bhashyam, A. R., Cervo, M., Kitada, T., Glass, K., Owen, C. A., Mahmood, A., Washko, G. R., Hashimoto, S., Ryter, S. W., and Choi, A. M. (2014). Mitophagy-dependent necroptosis contributes to the pathogenesis of COPD. *J Clin Invest* **124**, 3987-4003.

Nahak, B. K., Mishra, A., Preetam, S., and Tiwari, A. (2022). Advances in Organ-on-a-Chip Materials and Devices. *ACS Appl Bio Mater* **5**, 3576-3607.

Oh, J. M., Gangadaran, P., Rajendran, R. L., Hong, C. M., Lee, J., and Ahn, B. C. (2022). Different Expression of Thyroid-Specific Proteins in Thyroid Cancer Cells between 2-Dimensional (2D) and 3-Dimensional (3D) Culture Environment. *Cells* **11**.

Pearce, E. L., Poffenberger, M. C., Chang, C. H., and Jones, R. G. (2013). Fueling immunity: insights into metabolism and lymphocyte function. *Science* **342**, 1242454.

Prakash, Y. S., Pabelick, C. M., and Sieck, G. C. (2017). Mitochondrial Dysfunction in Airway Disease. *Chest* **152**, 618-626.

Prasad, S., Gupta, S. C., and Tyagi, A. K. (2017). Reactive oxygen species (ROS) and cancer: Role of antioxidative nutraceuticals. *Cancer Lett* **387**, 95-105.

Ramadan, Q., and Gijs, M. A. (2015). In vitro micro-physiological models for translational immunology. *Lab Chip* **15**, 614-36.

Rastrick, J. M., Stevenson, C. S., Eltom, S., Grace, M., Davies, M., Kilty, I., Evans, S. M., Pasparakis, M., Catley, M. C., Lawrence, T., Adcock, I. M., Belvisi, M. G., and Birrell, M. A. (2013).

Cigarette smoke induced airway inflammation is independent of NF-κB signalling. *PLoS One* **8**, e54128.

Richter, A., O'Donnell, R. A., Powell, R. M., Sanders, M. W., Holgate, S. T., Djukanović, R., and Davies, D. E. (2002). Autocrine ligands for the epidermal growth factor receptor mediate interleukin-8 release from bronchial epithelial cells in response to cigarette smoke. *Am J Respir Cell Mol Biol* **27**, 85-90.

Robinson, N. B., Krieger, K., Khan, F. M., Huffman, W., Chang, M., Naik, A., Yongle, R., Hameed, I., Krieger, K., Girardi, L. N., and Gaudino, M. (2019). The current state of animal models in research: A review. *Int J Surg* **72**, 9-13.

Romagna, G., Allifranchini, E., Bocchietto, E., Todeschi, S., Esposito, M., and Farsalinos, K. E. (2013). Cytotoxicity evaluation of electronic cigarette vapor extract on cultured mammalian fibroblasts (ClearStream-LIFE): comparison with tobacco cigarette smoke extract. *Inhal Toxicol* **25**, 354-61.

Shuler, M. L. (2017). Organ-, body- and disease-on-a-chip systems. *Lab Chip* **17**, 2345-2346.

Tang, X., Li, Z., Yu, Z., Li, J., Zhang, J., Wan, N., Zhang, J., and Cao, J. (2021). Effect of curcumin on lung epithelial injury and ferroptosis induced by cigarette smoke. *Hum Exp Toxicol* **40**, S753-s762.

Vayssier-Taussat, M., Camilli, T., Aron, Y., Meplan, C., Hainaut, P., Polla, B. S., and Weksler, B. (2001). Effects of tobacco smoke and benzo[a]pyrene on human endothelial cell and monocyte stress responses. *Am J Physiol Heart Circ Physiol* **280**, H1293-300.

Vayssier, M., Banzet, N., François, D., Bellmann, K., and Polla, B. S. (1998). Tobacco smoke induces both apoptosis and necrosis in mammalian cells: differential effects of HSP70. *Am J Physiol* **275**, L771-9.

Wallace Hayes, A., Muriana, A., Alzualde, A., Fernandez, D. B., Iskandar, A., Peitsch, M. C., Kuczaj, A., and Hoeng, J. (2020). Alternatives to Animal Use in Risk Assessment of Mixtures. *Int J Toxicol* **39**, 165-172.

Wang, H., Chen, H., Huang, L., Li, X., Wang, L., Li, S., Liu, M., Zhang, M., Han, S., Jiang, X., Fu, Y., Tian, Y., Hou, H., and Hu, Q. (2021). In vitro toxicological evaluation of a tobacco heating product THP COO and 3R4F research reference cigarette on human lung cancer cells. *Toxicol In Vitro* **74**, 105173.

Wang, M., Zhang, Y., Xu, M., Zhang, H., Chen, Y., Chung, K. F., Adcock, I. M., and Li, F. (2019). Roles of TRPA1 and TRPV1 in cigarette smoke -induced airway epithelial cell injury model. *Free Radic Biol Med* **134**, 229-238.

Wang, Z., White, A., Wang, X., Ko, J., Choudhary, G., Lange, T., Rounds, S., and Lu, Q. (2020). Mitochondrial Fission Mediated Cigarette Smoke-induced Pulmonary Endothelial Injury. *Am J Respir Cell Mol Biol* **63**, 637-651.

Xiao, R. R., Jing, B., Yan, L., Li, J., Tu, P., and Ai, X. (2022). Constant-rate perfused array chip for high-throughput screening of drug permeability through brain endothelium. *Lab Chip* **22**, 4481-4492.

Xiao, R. R., Lv, T., Tu, X., Li, P., Wang, T., Dong, H., Tu, P., and Ai, X. (2021). An integrated biomimetic array chip for establishment of collagen-based 3D primary human hepatocyte model for prediction of clinical drug-induced liver injury. *Biotechnol Bioeng* **118**, 4687-4698.

Yamada, K. M., and Cukierman, E. (2007). Modeling tissue morphogenesis and cancer in 3D. *Cell* **130**, 601-10.

Zhang, M. Y., Jiang, Y. X., Yang, Y. C., Liu, J. Y., Huo, C., Ji, X. L., and Qu, Y. Q. (2021). Cigarette smoke extract induces pyroptosis in human bronchial epithelial cells through the ROS/NLRP3/caspase-1 pathway. *Life Sci* **269**, 119090.

Zhao, Z., Wang, X., Zhang, R., Ma, B., Niu, S., Di, X., Ni, L., and Liu, C. (2021). Melatonin attenuates smoking-induced atherosclerosis by activating the Nrf2 pathway via NLRP3 inflammasomes in endothelial cells. *Aging (Albany NY)* **13**, 11363-11380.

Graphical abstract

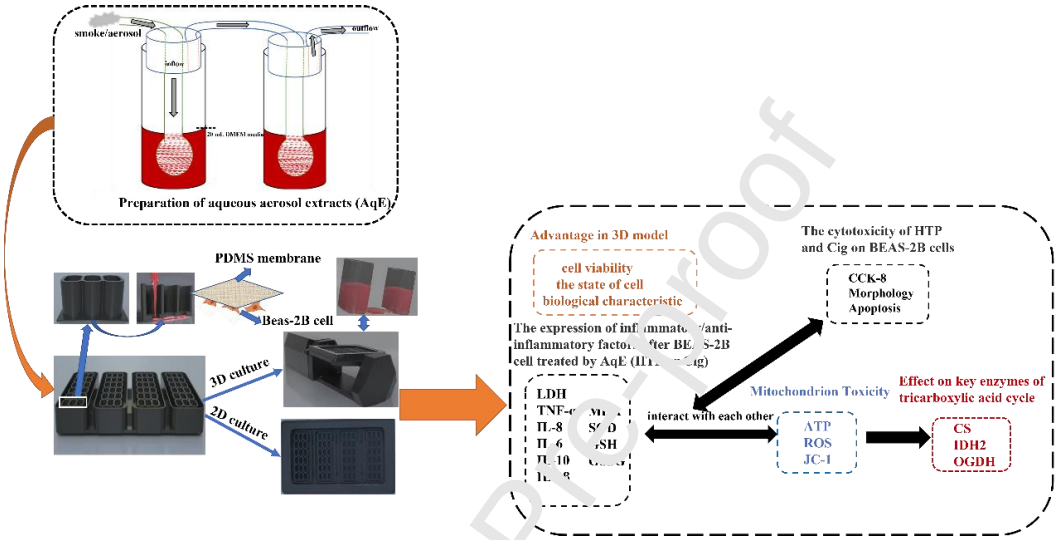

Schematic overview of the experimental design. (A) Preparation of aqueous aerosol extracts. (B) 3D chip model construction and working principle. (C) Detailed experimental evaluation.

Suppl Table 1 Aerosol generation regimens and nicotine levels in test product AqE.

Product	Puff regimen	Puff Volume (mL)	Puff Frequency (seconds)	Puff Duration (seconds)	Nicotine (μg/mL)	SD.
HTP	HCI	55	30	2	17.48	1.34
Cig	HCI	55	30	2	26.32	2.26

Nicotine was captured in the AqEs from Cigarette smoke (Cig) and Heated Tobacco Product (HTP) aerosols. Data shown are mean (± standard deviation (SD.) of 6 individual batches of AqE for each test product. Abbreviation: HCI, HCI T-115 (World Health Organization, 2015), AqE, Aqueous extracts.

Suppl Table 2 Calculated nicotine levels in test product AqE exposure concentrations.

HTP			Cig		
Aqe stock (%)	AqE puffs/mL	Nicotine (μg/mL)	Aqe (%)	AqE puffs/mL	Nicotine (μg/mL)
100	0.5	17.48	100	0.5	26.32
50	0.25	8.74	50	0.25	13.16
25	0.125	4.37	25	0.125	6.58

Nicotine concentrations were calculated on the assumption of linear dilution of nicotine in the AqE.

Declaration of interests

☒ The authors declare that they have no known competing financial interests or personal relationships that could have appeared to influence the work reported in this paper.

☐The authors declare the following financial interests/personal relationships which may be considered as potential competing interests:

Highlights

1) The in vitro 3D biomimetic chip model was used to better evaluate the controversial heated cigarette products, which solved the shortcomings of two-dimensional cell culture and animal models.
2) It is more obvious that the toxicity of traditional cigarettes is much higher than that of heated cigarette products, and the toxicity of cigarette extract diluted four times under the same number of puffs is higher than that of undiluted heated cigarettes. Both tobacco products cause oxidative stress damage to mitochondria, which may affect the tricarboxylic acid cycle in energy metabolism.
3) This study provides the necessary important data for risk assessment, proving that HTP may be less harmful than tobacco cigarettes, but it does show significant cytotoxicity with the increase of dosage.